ISBN: 978-3-95450-227-1 ISSN: 2673-5490 doi:10.18429/JACoW-IPAC2022-THPOTK002

MAGNET DESIGN FOR THE PETRA IV STORAGE RING

I. Agapov, A. Aloev†, R. Bartolini, H.-J. Eckoldt, D. Einfeld, B. Krause,
A. Petrov, M. Thede, M. Tischer, DESY, Hamburg, Germany
J. Chavanne, ESRF, Grenoble, France

Abstract

The proposed PETRA IV electron storage ring that will replace DESY's flagship synchrotron light source PETRA III will feature a horizontal emittance as low as 20 pmrad. It is based on a hybrid six-bend achromat lattice. In addition to the storage ring PETRA IV, the Booster Synchrotron and the corresponding transfer line will be renewed.

Overall about 4000 magnets will be manufactured. This contribution presents the electromagnetic design of the magnets for the storage ring.

INTRODUCTION

DESY is currently producing the Technical design for the PETRA IV upgrade [1] with the aim of replacing the existing PETRAIII ring with a new ultra-low emittance storage ring based on a modified H6BA lattice [2]. The new storage ring will be built in the same tunnel 2.3 km long with the eight octants structure of the original PETRA collider. The nominal emittance of 20 pm is achieved by a using a H6BA cell structure repeated nine times per octant and the extensive use of damping wigglers in five of the eight octants of the ring. The basic cell is based on a quadrupole triplet at each end to control the optics function at the straight sections, on six combined function bending magnets and two dispersions bumps at π degrees phase advance to control the chromaticity correction. Octupoles are used to control the nonlinear beam dynamics. In total each cell hosts two longitudinal combined-function dipoles, four combined-function dipoles, 17 quadrupoles, 6 sextupoles, and 7 correctors. A layout of the H6BA cell with the location of the magnet is shown in Fig. 1

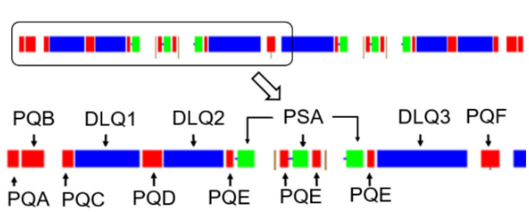

Figure 1: location of the magnetic element in the H6B cell: quadrupoles (red), sextupoles (green), dipoles (blue).

The dipoles will be built with permanent magnets while all the other magnets will be resistive. That reduces overall power consumption of the magnets to 1.2 MW. In this paper we report the current status of the design of the main magnetic elements highlighting the main challenges.

† alexander.aloev@desy.de

NORMAL CONDUCTING MAGNETS

Quadrupole Magnets

The PETRA IV lattice requires relatively high gradient quadrupoles to control the optics function in particular at the triplet of the straight sections. The main parameters of the quadrupoles are reported in Table. 1 with the corresponding field quality specifications provided by beam physics simulations. Significant effort has been put not only in providing the required field quality at high gradients, but also in minimising the power consumption.

The PQA, PQB, PQD and PQE quadrupole families would be unfeasible with conventional yoke material, such as Armco, due to the yoke saturation, caused not only by high gradients, but also by short magnet lengths. In order to reach the required gradient values and to reduce power consumption, these magnets were designed with pole tips, made of high permeability material (Vacoflux 50) and the rest of the yoke with Armco. This approach had been implemented and tested in APS-U magnets [3].

Table 1: Parameters of Designed PETRA IV Quadrupoles

Type	PQA	PQB	PQC	PQD	PQE	PQF	PQH
Gradient, T/m	115	112	86	97	91	83	86
Magnetic length, mm	169	345	161	280	110	250	300
Aperture radius, mm	11.0	11.0	12.5	12.5	12.5	12.5	12.5
Pole to pole clearance, mm	8.8	8.8	10.0	11.0	10.0	10.0	10.0
GFR, mm	6.5	6.5	7.9	7.9	7.9	7.9	7.9
Field harmonics $\sqrt{\Sigma b_n^2}$				$< 5\times10^{-4}$			
Operational gradient range, %				± 5 %			
Power, kW	0.9	1.4	0.7	1.6	0.7	0.9	1.2
Quantity	128	128	128	144	576	86	14

Even with the high-permeability pole tips, the PQA and PQB aperture radius had to be reduced from 12.5 to 11.0 mm. PQB quadrupole power loss would be 2.4 kW with laminated Powercore 1400 yoke and is only 1.4 kW with Vacoflux 50 pole tips.

Yoke geometries were optimised to maximise the gradients and the field quality and at the same time to minimise volume of the high-permeability poles. Due to short length of the magnets, transverse cross-sections were optimised

ISBN: 978-3-95450-227-1 ISSN: 2673-5490 doi:10.18429/JACoW-IPAC2022-THPOTK002

first in 2D and then in 3D. A 3D layout of the PQE quadrupole is shown in Fig. 2

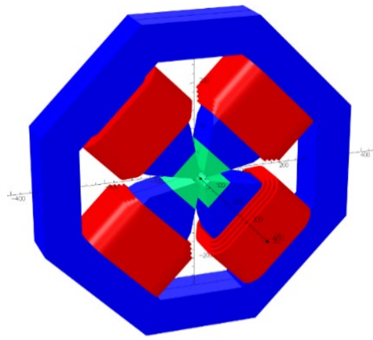

Figure 2: PQE quadrupole with coils (red), Vacoflux pole tips (green) and Armco yoke (blue).

The excitation curve of the PQE quadrupole is shown in Fig. 3, from which it is clear that a single material yoke (e.g. ARMCO) would operate in a strongly saturated regime, making the design very inefficient.

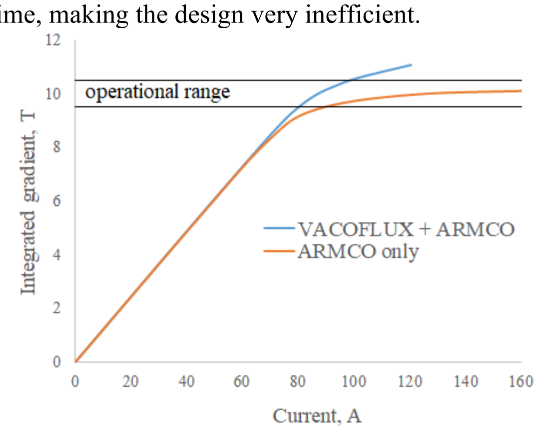

Figure 3: PQE excitation curve.

The PQD quadrupole requires an increased pole to pole clearance to allow the extraction of the photon pipe, which makes the pole tip relatively narrow. The pole profile, shown in Fig. 4, allows supressing 6th and 10th harmonics and makes the 6th harmonics less dependent on saturation effects at different excitation currents. In colour is the relative permeability map at the pole. Figure 5 reports the PQD harmonics.

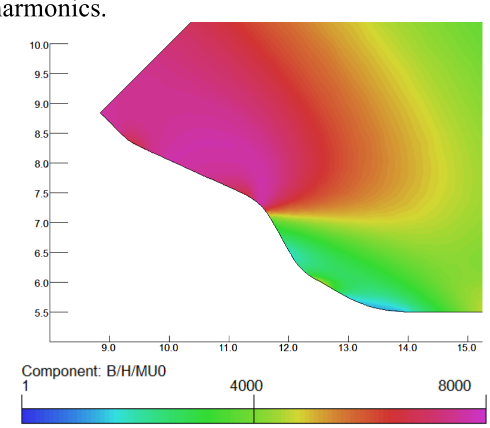

Figure 4: PQD pole profile details.

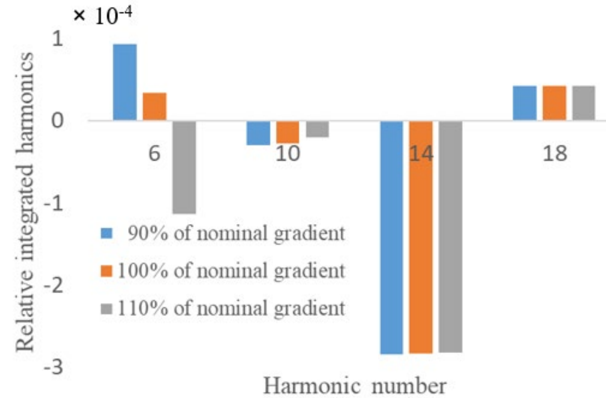

Figure 5: PQD relative integrated harmonics at 7.9 mm radius (63% of the aperture) at different excitation levels.

Sextupole and Octupole Magnets

The PETRA IV sextupoles follow a conventional design with integrated coils for vertical and horizontal correction and skew quadrupole correctors. The octupole follows the layout of ESRF-EBS octupole, consisting of fours separate yoke parts and four coils. This configuration allows wider pole to pole clearance [4].

Table 2: Parameters of Designed PETRA IV Sextupole and Octupole

	PSA Sextupole	POA Octupole
Gradient	2 700 T/m^2	120 000 T/m^3
Magnetic length, mm	250	90
Aperture radius, mm	12.5	
GFR, mm	7.9	
Field harmonics $\sqrt{\Sigma b_n^2}$	$< 5{\times}10^{-4}$	

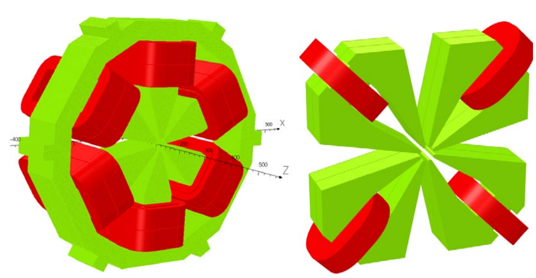

Figure 6: PSA sextupole and POA octupole.

Combined Corrector Magnets

PETRA IV combined AC/DC horizontal and vertical correctors deflect the beam up to 800 µrad. The design is based on 8-pole corrector magnet for APS-U [3].

Each of the poles holds two coils – main and auxiliary. Main and auxiliary coils for one deflection direction are connected in series. At a certain ratio of conductor turns in these coils it is possible to minimise 3rd and 5th harmonics. The number of turns is also chosen to meet the power supply requirements for maximum current and inductance.

ISBN: 978-3-95450-227-1 ISSN: 2673-5490 doi:10.18429/JACoW-IPAC2022-THPOTK002

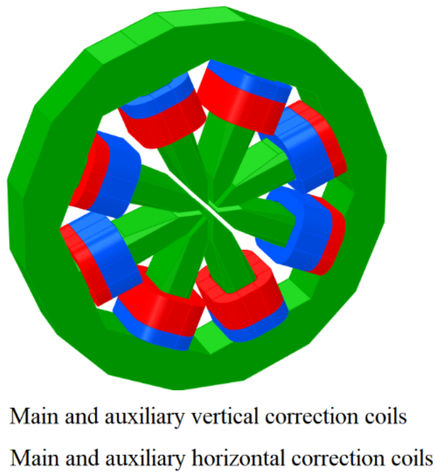

Figure 7: Combined corrector.

COMBINED-FUNCTION DIPOLES

Following the successful operation of permanent magnet based dipoles at the ESRF-EBS [5], the PETRA IV design will further elaborate this concept. All dipoles will additionally have a moderate quadrupole gradient which is realised by a slanted pole design in a C-shape geometry. The parameters of all DLQ magnets are shown in Table 3. DLQ1 also provides a longitudinal gradient with a fixed ratio G/B which is made in 4 steps similar to the DL magnets of the ESRF-EBS. The design is done in a modular, largely unified way, the specified field amplitude is obtained by a matched filling of the permanent magnet slots whereas the correct gradient is achieved by the particular pole shape. Due to higher radiation hardness, SmCo is used as permanent magnet material while yoke and poles are made of Armco. The magnets have an overall cross-section of about 120x200 mm^2 and will be mounted on an adjustable support base.

Table 3: Parameters of the Combined-Function Dipoles

	Magn. Length, m	Field, T	Gradient, T/m
DLQ1	0.303	0.287	11.69
	0.303	0.277	11.27
	0.303	0.255	10.39
	0.303	0.223	9.09
DLQ2	1.084	0.191	7.81
DLQ3	1.818	0.193	6.63

All DLQs will be built of 4-6 straight modules which will be placed to each other with a small angle (~1mrad) following the curved beam trajectory. A 2D optimisation of the cross-section and pole contour (Fig. 8) has been made for all DLQ types including appropriate thermal shims for temperature compensation and some margin for later shimming of the field. The resulting field performance is shown in Fig. 9; specifications on aperture, good-field radius, and residual harmonics correspond to those of most other magnets (Tab.2).

The 3D-optimisation of all DLQ types is ongoing presently and is realised by short, particularly shaped end-pole pieces. Figure 10 shows a full DLQ after optimisation. In parallel, the mechanical design of the DLQ is progressing in order to launch a first prototype in the near future.

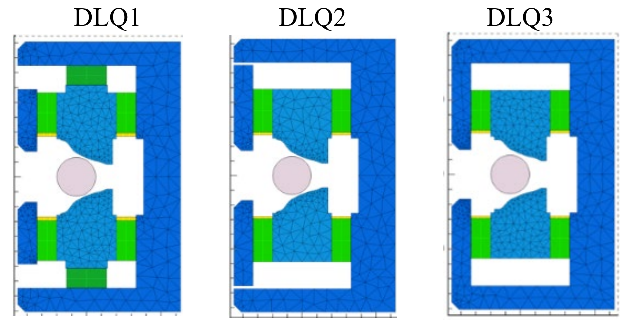

Figure 8: Cross sections of combined-function dipoles; thermal shims (yellow) are placed on top of the permanent magnets (green).

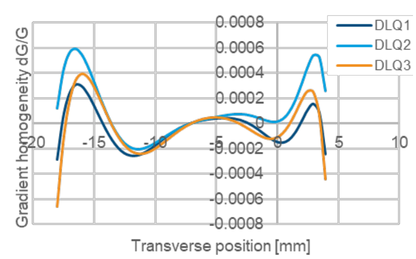

Figure 9: Gradient homogeneity of 2D-optimised pole profiles. The centre of the good-field region is located about 7 mm towards the open side of the magnets.

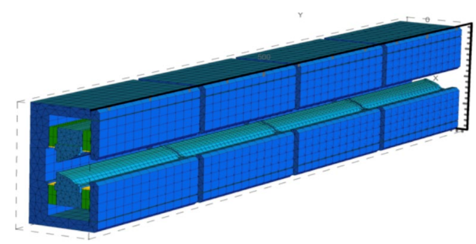

Figure 10: The single straight modules of a full dipole will be canted by ~1mrad with respect to each other.

REFERENCES

[1] R. Bartolini *et al.*, "Status of the PETRA IV Project", presented at the IPAC'22, Bangkok, Thailand, Jun. 2022, paper TUPOMS029, this conference.

[2] I. V. Agapov *et al.*, "PETRA IV Storage Ring Design", presented at the IPAC'22, Bangkok, Thailand, Jun. 2022, paper TUPOMS014, this conference.

[3] M. Jaski, "APS Upgrade: Magnets", ASD Seminar, Apr. 2017

[4] C. Benabderrahmane *et al.*, "Magnets for the ESRF-EBS Project", in *Proc. IPAC'16*, Busan, Korea, May 2016, pp. 1096-1099. doi:10.18429/JACoW-IPAC2016-TUPMB001

[5] C. Benabderrahmane *et al.*, "Status of the ESRF-EBS Magnets", in *Proc. IPAC'18*, Vancouver, Canada, Apr.-May 2018, pp. 2648-2651. doi:10.18429/JACoW-IPAC2018-WEPMK009